

Investigation of the Ductile-to-Brittle Transition during Scratching of Polycrystalline Dual-phase γ -TiAl Alloy

Ailin Liu *

College of Mechanical Engineering, Tianjin University of Technology and Education, Tianjin, China

* Corresponding Author Email: liuailin9888@163.com

ABSTRACT

This study investigates the ductile-to-brittle transition (DBT) in a polycrystalline dual-phase γ -TiAl alloy through a novel variable-depth, variable-speed scratch testing approach. Continuous grooves (0–40 μm) were created at scratching speeds of 500–4000 mm/min using a diamond conical indenter, with in-situ cutting forces monitored via a Kistler dynamometer and surface morphologies captured using synchronized 3D optical and confocal laser scanning microscopy. The results delineate three distinct deformation regimes: (1) ductile material removal (< 6–7 μm), characterized by smooth surfaces and stable forces; (2) a mixed-mode transition zone (6–14 μm), marked by microcrack initiation and periodic force oscillations; and (3) brittle-dominated fracture (> 14–16 μm), exhibiting extensive cracking and pronounced force fluctuations. Higher scratching speeds amplified force amplitudes and accelerated crack onset. Critical uncut chip thicknesses for DBT onset and completion were quantified at 6–7 μm and 14–16 μm , respectively. This work provides the synchronized mechanical–morphological analysis of DBT in γ -TiAl at the microscale, offering quantitative insights for optimizing high-speed micromachining processes and enhancing surface integrity in aerospace applications.

KEYWORDS

γ -TiAl Alloy; Ductile-to-brittle Transition; High-speed Scratch; Cutting Force; Surface Morphology.

1. INTRODUCTION

γ -Titanium aluminide (γ -TiAl) alloys are prized for their low density, high specific strength, and excellent high-temperature oxidation resistance, making them ideal for aerospace applications such as turbine blades and engine components [1],[2]. However, their limited room-temperature ductility and propensity for crack initiation at γ/α_2 phase interfaces pose significant challenges in precision machining, often compromising surface quality and component performance. Understanding the ductile-to-brittle transition (DBT) during material removal is critical to optimizing machining parameters and enhancing the service life of γ -TiAl components.

Scratch testing is widely recognized as an effective method for investigating DBT phenomena, owing to its precise control over undeformed chip thickness, real-time force monitoring capability, and the elimination of sample-to-sample variability. Prior studies have made valuable contributions: for instance, Zhang et al. [3] employed depth-variable scratch tests with wavelet analysis to study crack evolution in single-crystal γ -TiAl, and Feng et al. [4] conducted molecular dynamics simulations to assess the effects of indenter geometry and crystallographic orientation. However, most existing studies either focus on single-speed or single-depth conditions or lack synchronous macro–micro characterization. As such, they fall short of capturing the complete spectrum of DBT behavior in polycrystalline dual-phase γ -TiAl.

This study introduces a novel variable-depth, variable-speed scratch testing methodology, integrating in-situ force measurements with synchronized 3D optical and confocal microscopy. By generating continuous grooves (0–40 μm) at speeds of 500–4000 mm/min, we quantitatively map the DBT process, identifying critical chip thicknesses and speed-dependent deformation mechanisms. This work provides a comprehensive framework for optimizing high-speed micromachining of γ -TiAl alloys, offering practical guidance for improving surface integrity in advanced manufacturing applications. [5].

2. EXPERIMENTAL MATERIALS AND METHODS

2.1. Material characterisation

The material investigated was a polycrystalline dual-phase γ -TiAl alloy whose chemical composition is listed in Table 1. Phase identification and quantitative analysis were performed on a Rigaku ZSX Primus III+ wavelength-dispersive X-ray fluorescence spectrometer (50 kV, 60 mA). The alloy ingots were prepared by vacuum induction melting (VIM) using high-purity raw materials under argon protection with multiple remelts to ensure chemical homogeneity and dense microstructure. Post-casting, the ingots underwent hot isostatic pressing (HIP) at 1250 °C and 150 MPa for 3 h to eliminate internal porosity, followed by a two-stage homogenization heat treatment at 1280 °C for 1.5 h and 900 °C for 6 h to promote $\alpha \rightarrow \alpha_2 + \gamma$ eutectoid transformation and refine the lamellar structure. Finally, furnace cooling was applied to minimize residual stresses and optimize high-temperature performance. The resulting microstructure comprised Near-Gamma, Duplex, Near-Lamellar, and Fully-Lamellar regions, with the Fully-Lamellar morphology characterized by alternating γ (TiAl) and α_2 (Ti_3Al) lamellae (Fig. 1). Test specimens were machined to dimensions of 18 \times 13 \times 8 mm. Their mechanical properties are summarized in Table 2.

Table 1. Chemical composition of γ -TiAl alloy

| Elements | Al(mass%) | Si(mass%) | Ti(mass%) | V(mass%) | Mn(mass%) | Nb(mass%) |
|----------|-----------|-----------|-----------|----------|-----------|-----------|
| Content | 28.8024 | 0.0278 | 62.9277 | 0 | 2.9799 | 5.2611 |

Table 2. Mechanical properties

| Poisson's ratio | Elongation (%) | Density (g/cm^3) | Tensile strength (MPa) | Yield strength (MPa) | Elastic modulus (GPa) | Fracture toughness ($\text{MPa}\cdot\text{m}^{1/2}$) |
|-----------------|----------------|------------------------------------|------------------------|----------------------|-----------------------|--------------------------------------------------------|
| 0.26 | 1.5 | 4.12 | 970 | 770 | 166 | 15 |

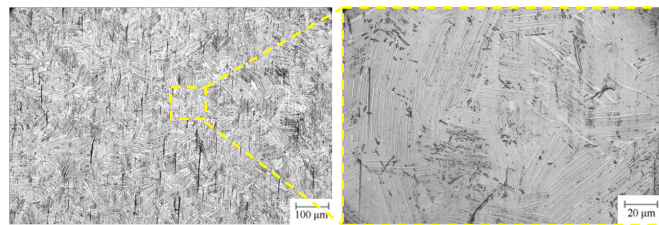


Figure 1. Micrograph of γ TiAl alloy

2.2. Experimental Design and Characterisation Methods

In the variable-depth scratch test, a diamond conical tool was used to cut along the Y-direction of the sample surface, with the cutting depth gradually increasing from 0 to 40 μm (Fig. 2), resulting in a groove with continuously varying depth. To minimize the influence of sample variability and clamping errors, five sets of scratch tests at different sliding speeds were conducted sequentially on

the same specimen (Table 3). Due to the short duration of each scratch, tool wear was negligible, enhancing experimental efficiency and reducing costs. This method, commonly applied to brittle materials, allows precise identification of the ductile-to-brittle transition depth.

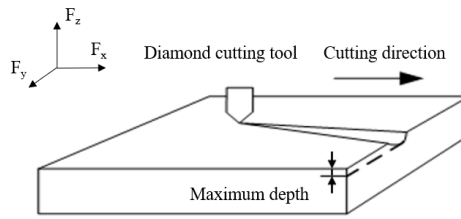


Figure 2. Schematic diagram of variable cutting depth

Table 3. Scratch parameters

| Experimental parameters | Parameter values |
|---------------------------------|-----------------------------|
| Scratch length (mm) | 7 |
| Scratch depth (μm) | 0-40 |
| Scratch speed (mm/min) | 500, 1000, 2000, 3000, 4000 |

3. EXPERIMENTAL RESULTS

3.1. Changes in Cutting Force

Figure 3 presents the evolution of three-directional cutting forces (F_x , F_y , F_z) during variable-depth scratching of γ -TiAl alloy at different scratching speeds. As the cutting depth increased, all force components rose rapidly and dropped sharply upon tool exit. Among them, the normal force F_z was dominant, followed by the tangential force F_x , while the lateral force F_y remained minimal. Higher scratching speeds led to larger F_z and F_x peaks and more fluctuating force curves. At lower speeds, the cutting force remained stable, indicating that material removal was primarily governed by plastic deformation. In contrast, higher speeds induced pronounced force fluctuations, suggesting an enhanced contribution from brittle fracture mechanisms. These results demonstrate that the ductile-to-brittle transition in γ -TiAl alloys is highly sensitive to processing speed[6].

Force profiles at different scratching speeds indicate that speeds above 2000 mm/min exhibit a distinct ductile-to-brittle transition. Figure 4 shows the evolution of normal and tangential forces with increasing cutting depth during scratching at 4000 mm/min. Both force components generally increase with depth, while the frequency and amplitude of force oscillations also intensify, reflecting significant changes in material removal behavior. Based on the force signal characteristics, the scratching process can be divided into three distinct stages:

- (1) Plastic cutting stage: At shallow depths during initial tool contact, material is primarily removed through plastic flow. Continuous chips are formed, cutting forces increase smoothly, and signal fluctuations are minimal.
- (2) Transition stage (ductile-to-brittle): As the depth increases further, periodic force oscillations emerge, indicating the onset of localized cracking. The removal mechanism begins to shift from continuous plastic deformation to intermittent brittle fracture.
- (3) Brittle cutting stage: At greater depths, crack propagation intensifies, and fracture dominates material removal. Force fluctuations become significantly amplified and stabilize at a higher level, indicating a transition to an unstable brittle removal regime.

This three-stage evolution demonstrates the transition of γ -TiAl alloy from plastic- to brittle-dominated removal during high-speed scratching. These insights are critical for understanding the

underlying mechanisms of the ductile-to-brittle transition and for defining the processing stability window in advanced machining applications.

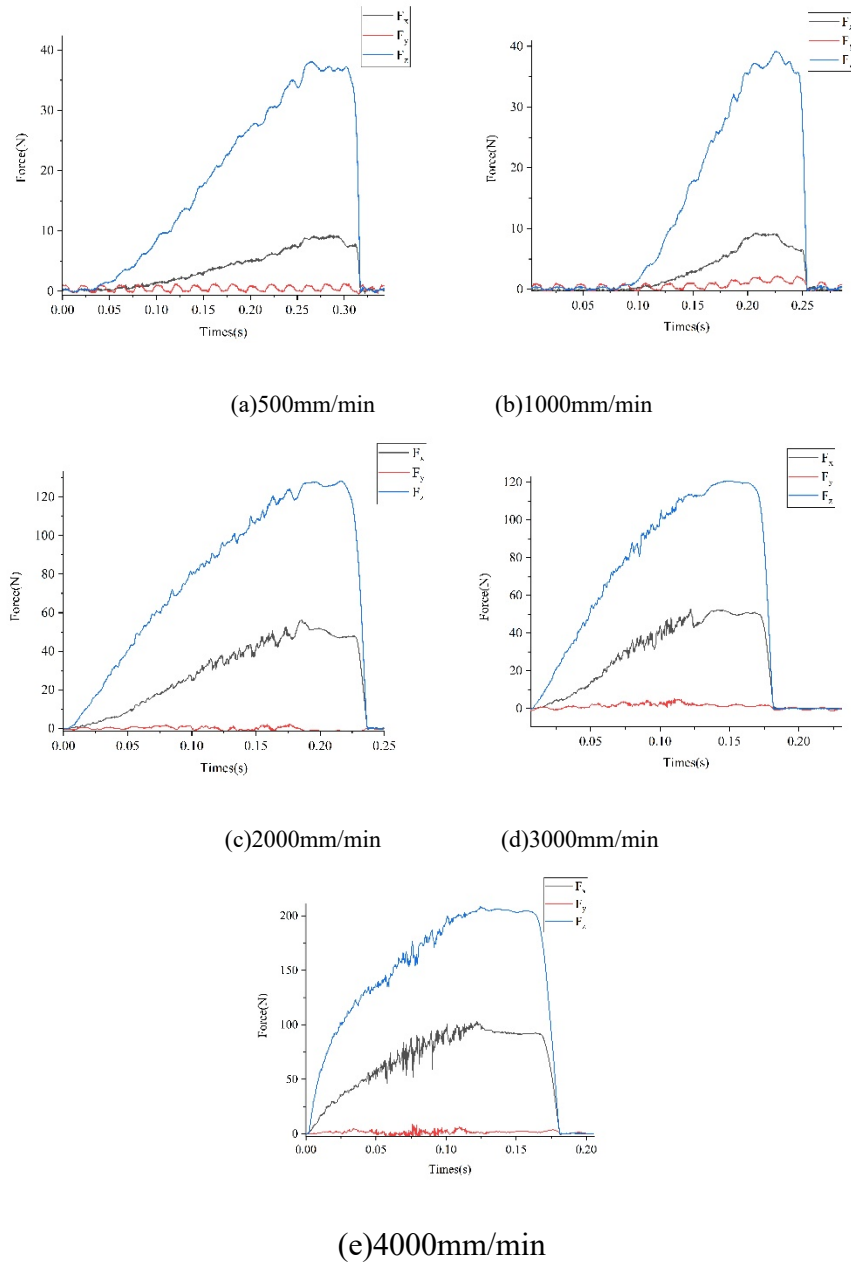


Figure 3. Cutting forces in the X, Y, and Z directions at different scratching speeds

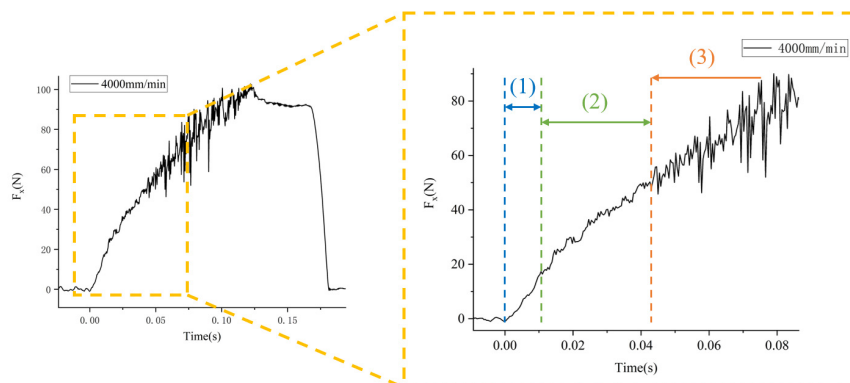


Figure 4. Curve showing the change in downward friction force over time at 4000 mm/min

Figure 5 presents the tangential and normal force profiles during scratching at five different speeds. A comparison of the peak cutting forces reveals that both tangential and normal forces increase with scratching speed. This indicates that, at the same cutting depth, higher scratching speeds lead to greater resistance to deformation in the γ -TiAl alloy.

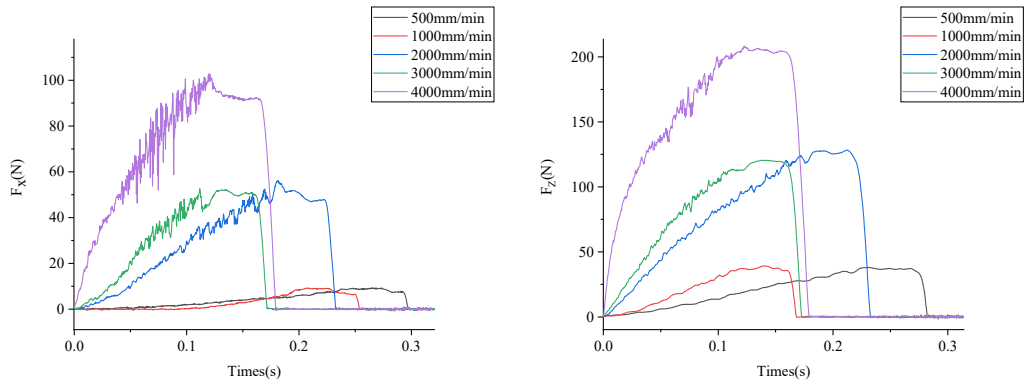


Figure 5. Cutting force curves for scratch processes at different scratch speeds

3.2. Surface Morphology Analysis of Scratches

From the force graph, it can be seen that experiments conducted at speeds above 2000 mm/min are more representative. Figure 6 illustrates the evolution of scratch surface features at different cutting depths under a speed of 2000 mm/min. As shown in Fig. 6(a), the overall groove widens progressively with increasing depth, indicating a corresponding increase in material removal volume. In the shallow region Fig. 6(b), aside from minor depressions caused by polishing, the scratch surface appears smooth and continuous, with no observable cracks or spalling. The furrow marks are well-defined and uniform, indicating a typical plastic cutting process at this stage. As the cutting depth increases, microcracks and small pits begin to appear within the scratch, suggesting enhanced local stress concentrations[7]. This marks a transition in the material removal mechanism from plastic deformation to the initial onset of brittle fracture, signifying the entry into the ductile-to-brittle transition stage.

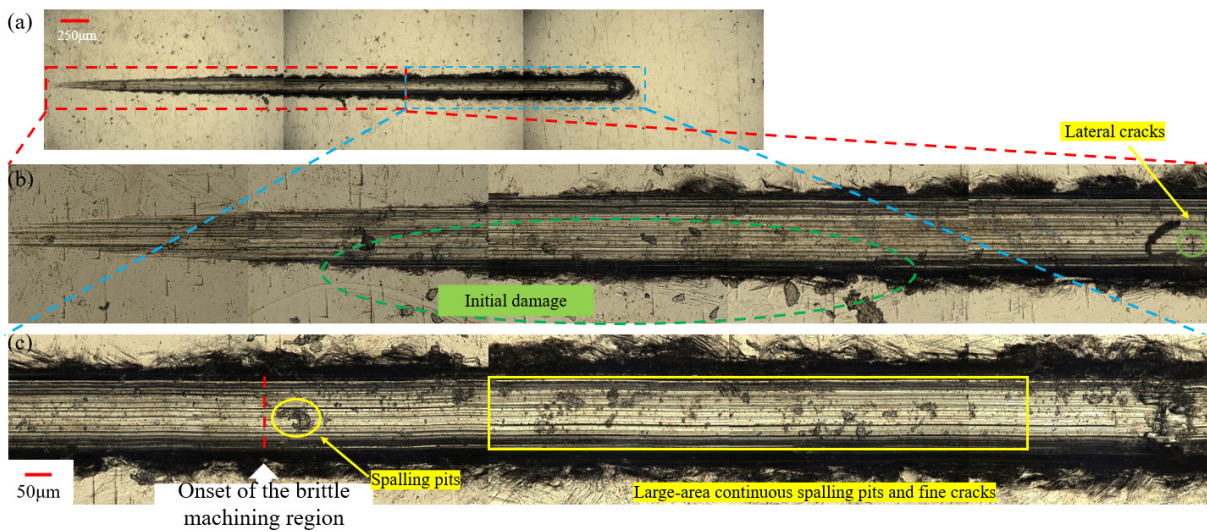


Figure 6. Surface morphology of scratches at a scratching speed of 2000 mm/min

Figure 6(c) illustrates that within the ductile-to-brittle transition zone, the scratch surface exhibits a random distribution of microcracks and small pits. Although the continuity of the ploughing grooves is somewhat reduced, the surface still retains characteristics of plastic material removal. As the cutting

depth increases further, larger pits begin to appear due to localized fracture or fragmentation. When the local stress or strain concentration exceeds the material's limit, cracks initiate and propagate through the surface or subsurface, ultimately intersecting and causing localized material detachment. This results in the formation of distinct "pit-like" structures. If these cracks propagate along lamellar interfaces, they tend to produce stepped delamination or deep pits.

At this stage, the surface shows a marked increase in both cracks and pits, and the discontinuous ploughing grooves suggest the onset of a fracture-dominated cutting regime. Overall, the transition from plastic to brittle deformation in γ -TiAl alloy is not abrupt but occurs gradually with increasing depth. This observation aligns with previous literature describing a progressive transition zone. Similar morphological evolution was observed across all scratch tracks in the experiment. Therefore, the depth at which pits and cracks begin to appear consistently is defined as the critical depth for brittle material removal.

Figure 7 presents the surface morphology evolution of scratches at a cutting speed of 3000 mm/min across different regions. In the plastic cutting zone, the scratch surface is smooth and free of cracks or pits, indicating that material removal is dominated by uniform plastic flow. In the middle of the transition zone, surface integrity declines, and isolated cracks, pits, and areas of plastic pile-up begin to emerge. This suggests a shift in the removal mechanism from plastic-dominated to brittle-dominated behavior. By the end of the transition zone, the surface is densely populated with fragmented pits and intersecting cracks, and the plastic ploughing marks are significantly reduced—hallmarks of brittle material removal. In summary, the material removal mechanism of γ -TiAl alloy evolves progressively from plastic to brittle with increasing depth, confirming a depth-dependent transition process.

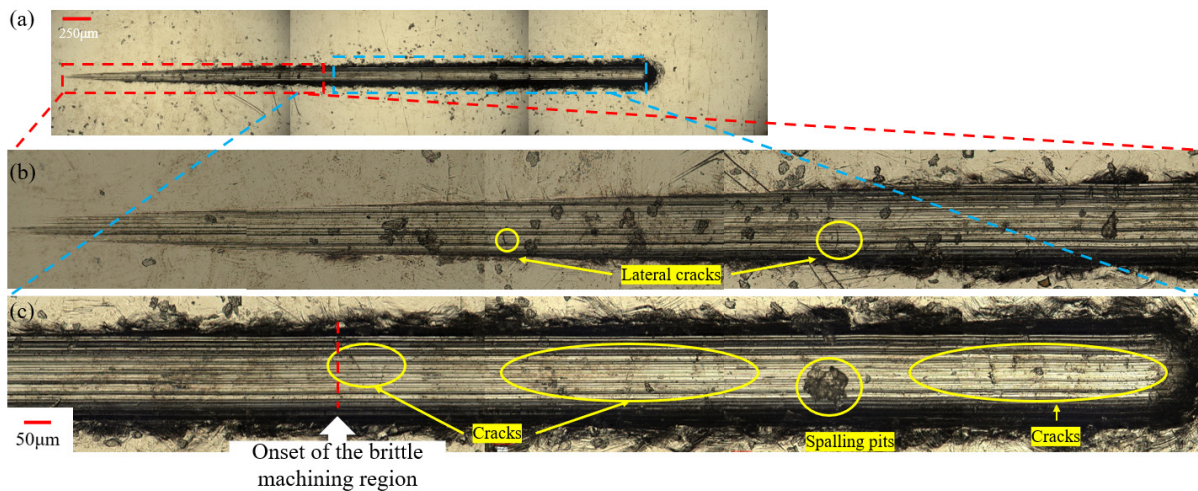


Figure 7. Surface morphology of scratches at a scratching speed of 3000 mm/min

As shown in Figure 8, additional evidence of brittle material removal can be observed at greater cutting depths, where more severe surface defects appear. Figure 8(c), captured using a 3D optical microscope, reveals prominent cracks located at the bottom of the scratch groove, indicating the occurrence of cleavage fracture on the surface. The γ -TiAl alloy features a fully lamellar microstructure composed of alternating γ (TiAl) and α_2 (Ti₃Al) phases, with relatively weak bonding at the lamellar interfaces. Under the applied scratching load, cracks tend to initiate or propagate along these interfaces. When the lamellae are oriented at specific angles to the scratching direction, crack propagation is further facilitated as the cracks "slip" onto the interfaces and extend along them.

As also observed in Figure 8, the cracks become significantly larger, and both the number and spread of fine cracks increase. γ -TiAl alloy is an inherently brittle intermetallic compound with extremely limited fracture ductility at room temperature. Unlike ductile metals, it has a limited capacity to absorb deformation energy through dislocation slip. Once the localized stress concentration exceeds

the crack initiation threshold, microcracks can readily form and rapidly propagate, eventually coalescing into large, continuous pits.

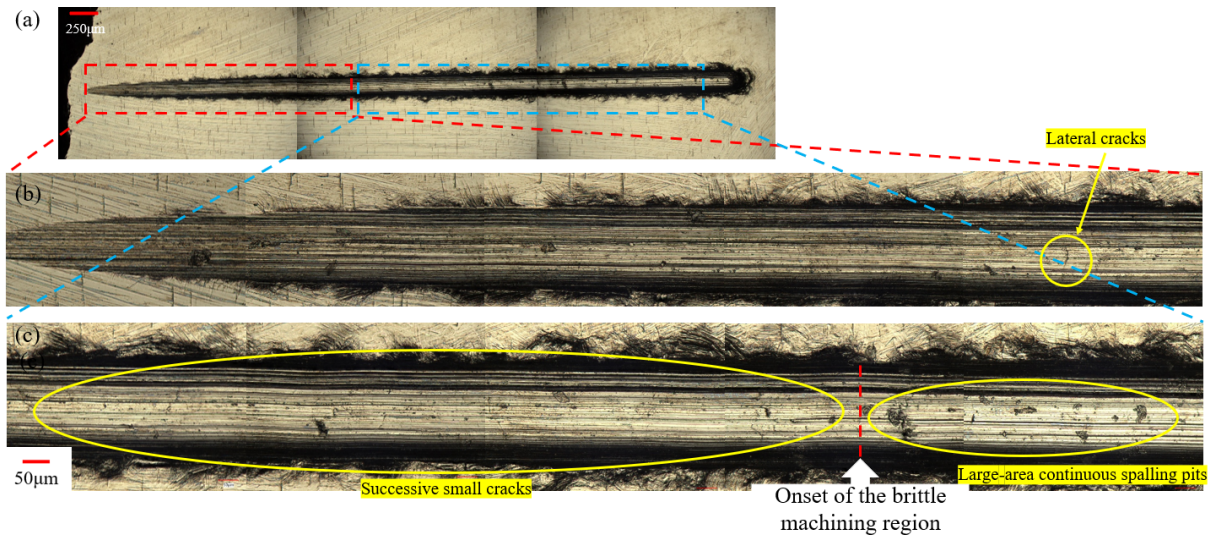


Figure 8. Surface morphology of scratches at a scratching speed of 4000 mm/min

These features indicate a pronounced brittle removal mechanism, characterized by a wide variety of complex surface defects. Such behavior likely explains the poor surface quality commonly observed in γ -TiAl machining.

3.3. Cutting Depth of the Ductile-to-brittle Transition Zone

The cutting depth corresponding to the ductile-to-brittle transition zone in the γ -TiAl alloy was determined based on the evolution of surface morphology with increasing scratch depth. As shown in Figure 9(a), the point at which continuous pits begin to appear on the scratch surface—accompanied by a noticeable change in the force signal curve—is identified as the end of the transition zone.

To locate the starting point of this transition, a 3D scratch profile was obtained using a confocal microscope. The corresponding location was then marked on the reconstructed surface morphology. At this point, the cross-sectional groove profile of the scratch was extracted, as illustrated in Figures 9(b), 9(f), and 9(i). The vertical distance between the groove profile and the reference baseline was measured and defined as the cutting depth at the onset of the ductile-to-brittle transition.

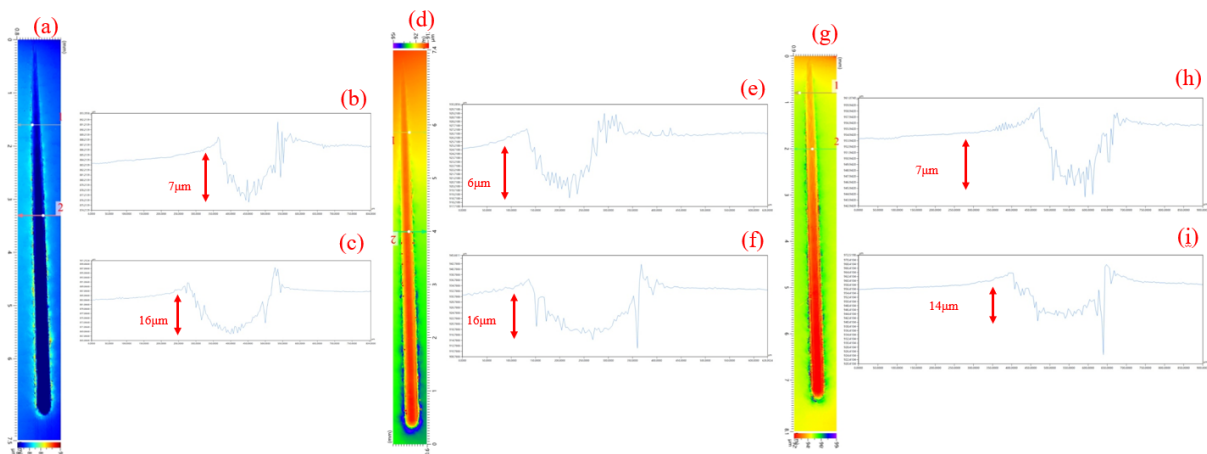


Figure 9. Method for obtaining the start and end depths of the brittle-ductile transition zone
 (a)(b)(c): 2000 mm/min (d)(e)(f): 3000 mm/min (g)(h)(i): 4000 mm/min

In summary, the uncut chip thickness corresponding to the plastic deformation zone and the transition zone in γ -TiAl alloy is approximately 6–7 μm , while that for the transition to the brittle cutting zone ranges from 14–16 μm . Based on scratch tests, the critical conditions for the ductile-to-brittle transition were identified. Analysis of surface morphology reveals that when the uncut chip thickness remains below approximately 16 μm , γ -TiAl alloy can be machined in a predominantly plastic mode, resulting in smooth surfaces without significant cracking.

Therefore, in subsequent conventional or ultrasonic milling processes, cutting parameters should be selected to maintain the uncut chip thickness below this critical threshold to significantly improve surface integrity. For conditions exceeding this value, process-assisted methods such as ultrasonic vibration are recommended to expand the ductile machining window and meet high-quality machining requirements[8].

4. SUMMARY

The variation in scratch depth of polycrystalline dual-phase γ -TiAl alloy can be divided into three zones: pure plastic zone ($< 6 \mu\text{m}$), ductile-to-brittle transition zone (6–14 μm), and brittle-dominated zone ($> 14 \mu\text{m}$), corresponding to the patterns of force fluctuations and surface crack morphology evolution.

- (1) Coupled mechanical and morphological mechanism: Within the transition zone, cutting force fluctuations occur simultaneously with the appearance of surface cracks and pits observed via extended depth-of-field microscopy. This reflects the concurrent instability of microcrack initiation and plastic deformation, ultimately leading to interfacial crack coalescence and block spallation.
- (2) Parameter sensitivity: Scratch speed significantly affects the peak force and the onset depth of force fluctuations. The uncut chip thickness is the critical parameter controlling plastic machining, with thresholds at approximately 6–7 μm and 14–16 μm .
- (3) Process guidance: To ensure high-quality surfaces, the uncut chip thickness should be controlled within 6–8 μm and moderate to low speeds are preferred. When necessary, vibration-assisted techniques can be introduced to suppress brittle crack propagation.

This study combines extended depth-of-field 3D imaging and confocal depth profiling to quantitatively characterize the ductile-to-brittle transition of γ -TiAl alloy at the micron scale for the first time, providing theoretical basis and quantitative guidance for the optimization of subsequent micromachining processes.

CONFLICTS OF INTEREST

The authors declare that they have no conflict of interest.

REFERENCES

- [1] Appel, F., Brossmann, U., Christoph, U., Eggert, S., Janschek, P., Lorenz, U., Müllauer, J., Oehring, M., & Paul, J. D. H. (2000). Recent progress in the development of gamma titanium aluminide alloys. *Advanced Engineering Materials*, 2(11), 699–720. [https://doi.org/10.1002/1527-2648\(200011\)2:11](https://doi.org/10.1002/1527-2648(200011)2:11).
- [2] Genç O, Unal R. Development of gamma titanium aluminide (γ -TiAl) alloys: A review[J]. *Journal of Alloys and Compounds*, 2022, 929: 167262. <https://doi.org/10.1016/j.jallcom.2022.167262>.
- [3] Zhang Z, Shi K, Shi Y, et al. Evolution mechanisms of the scratch-induced elastoplastic stress fields and crack damage in γ -TiAl alloys[J]. *Journal of Materials Research and Technology*, 2025, 34: 932-945. <https://doi.org/10.1016/j.jmrt.2024.12.075>.

- [4] Feng R, Xu H, Zhou B, et al. Numerical simulation of the effect of scratching parameters and crystal orientation on the surface scratching mechanism of single-crystal γ -TiAl alloy[J]. Precision Engineering, 2025. <https://doi.org/10.1016/j.precisioneng.2025.01.020>.
- [5] Wang Z, Liu Y. Study of surface integrity of milled gamma titanium aluminide[J]. Journal of Manufacturing Processes, 2020, 56: 806-819. <https://doi.org/10.1016/j.jmapro.2020.05.021>.
- [6] Zhang, T., Jiang, F., Huang, H., Lu, J., Wu, Y., Jiang, Z., & Xu, X. (2021). Towards understanding the brittle–ductile transition in the extreme manufacturing. International Journal of Extreme Manufacturing, 3(2), 022001. <https://doi.org/10.1088/2631-7990/abdfd7>.
- [7] Wu H, Zhang Y, Lu D, et al. Exploring the brittle-to-ductile transition and microstructural responses of γ -TiAl alloy with a crystal plasticity model incorporating dislocation and twinning[J]. Materials & Design, 2024, 246: 113360. <https://doi.org/10.1016/j.matdes.2024.113360>.
- [8] An W, Li Q, Gao X, et al. Non-synchronous ductile and brittle removal mechanisms for conventional and ultrasonic vibration-assisted scratching of ceramic matrix composites[J]. Composites Part A: Applied Science and Manufacturing, 2025, 190: 108718. <https://doi.org/10.1016/j.compositesa.2025.108718>.